

# Photo-induced and Dark Discharge Mechanisms of High Gamma Photoreceptors

Kuniki Seino, Hideaki Hirahara, Takaaki Konuma, Ichiro Yoshida and Shozo Kaieda, Afrit Corporation, Tokyo, Japan

## Abstract

An electrophotographic single layer organic photoreceptor consisting of relatively low concentrations of phthalocyanine pigments dispersed in an insulating binder polymer, which is generally referred to as a high gamma photoreceptor, shows the induction effect. Several mechanisms have been proposed to explain this phenomenon. However it is not completely clear at this time. In this paper, the photo-induced and dark discharge characteristics of the high gamma photoreceptors consisting of x-type metal-free phthalocyanine pigment and polyester polymer are found to be well described by our theoretical model which takes into account the structural trap. We have found that the good charge acceptance and the high gamma characteristics depend on structural traps. It is mathematically simulated that the x-type metal-free phthalocyanine's own photoresponse to digital image exposure is not deteriorated in spite of charge carrier trappings by structural traps during carrier transport.

## Introduction

Weigl reported in 1972 that an electrophotographic single layer organic photoreceptor consisting of relatively low concentrations of x-type metal-free phthalocyanine pigments dispersed in suitable binders, which is now referred to as a high gamma photoreceptor, shows the induction effect [1]. Kinoshita has proposed in 1989 to apply the induction effect to the photo-induced discharge by high intensity short pulse exposure in digital electrophotography [2, 3]. Since then, several mechanisms have been proposed to explain this unique phenomenon [4 - 7], however it is not completely clear at this time. In the present paper a theoretical model which takes into account the physical process of structural trap is applied to not only the photo-induced but also the dark discharge characteristics of high gamma photoreceptors.

## Experiment

The **Digital Photoreceptor HGPC** (High Gamma Photoreceptor) was fabricated with an electrophotographic single layer organic photoreceptor of 18 $\mu$ m thickness which consisted of x-type metal-free phthalocyanine (the average diameter: 0.7  $\mu$ m, 21.7 vol %) dispersed in low-molecular polyester on an 80 mm diameter aluminum drum. Hardness and moisture-fastness of the binder are improved by cross-linking a low molecular polyester with a molecular weight of about 5000 using butylated melamine resin. Photo-induced and dark discharge characteristics of **Digital Photoreceptor HGPC** are measured using the conventional PIDC method. The wavelength of exposure is 710 nm and the pulse exposure time is  $3.6 \times 10^{-3}$  sec. The amount of exposure is altered by changing the intensity of light source. The surface potential of

the photoconductive drum is measured after 0.3 sec from the pulse exposure.

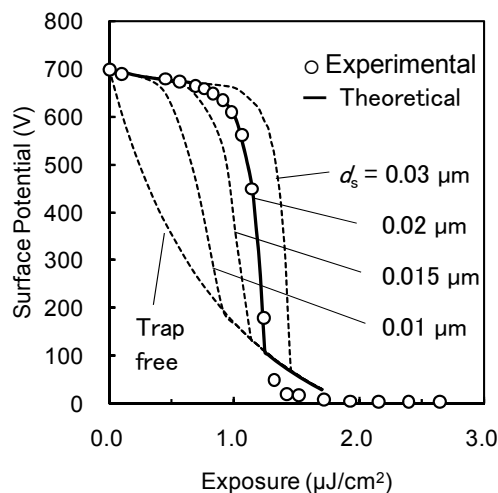


**Figure 1.** Photo-induced discharge characteristics for high gamma photoreceptor with x-type metal-free phthalocyanine. Solid line: theoretical curve calculated with structural depth  $d_s=0.02 \mu\text{m}$ . Broken lines: simulated curves calculated with various structural depths.

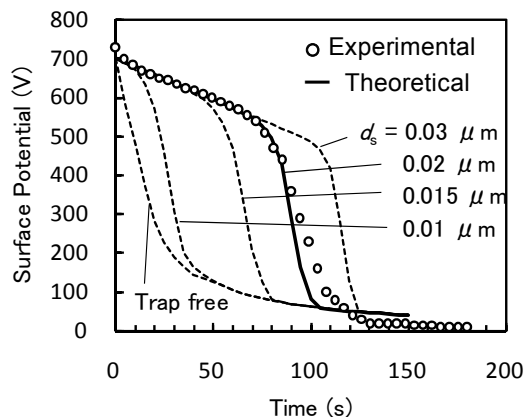


**Figure 2.** Dark discharge characteristics for high gamma photoreceptor with x-type metal-free phthalocyanine. Solid line: theoretical curve calculated with structural depth  $d_s=0.02 \mu\text{m}$ . Broken lines: simulated curves calculated with various structural depths.

## Result

**Fig. 1** shows the comparison between photo-induced discharge characteristics observed for **Digital Photoreceptor HGPC** and theoretical curve. The observed induction exposure is  $1.1 \mu\text{J}/\text{cm}^2$ .

Fig. 2 shows the comparison between dark discharge characteristics observed for **Digital Photoreceptor HGPC** and theoretical curve. The observed dark decay rate is about 2.5 V/sec and the slow dark decay period is about 80 sec.

## Discussion

### Structural trap model

Fig. 3 gives a schematic view of photoconductive particles randomly dispersing in an insulating binder polymer. Kitamura reported that the phthalocyanine pigments formed chains in the range of concentrations higher than 20 wt % of phthalocyanine pigment [6]. According to the percolation theory, endless chains are formed higher than 16 vol % of spherical bodies and those average contact points are to be 2.1. As is indicated in Fig. 3, under such circumstances that the contact point to the next particle is eccentrically from the center of the base of spherical bodies in the direction of electric field, free carriers are considered to be trapped within a saucer-shaped space surrounded by insulating binder polymer [8]. The distance from the base is termed a structural depth. The electric field due to surface charges generates electrostatic potential wells within the structural traps. Trapped carriers with kinetic energy higher than the energy barrier move to the next photoconductive particle through the contact point as is indicated by an arrow a.

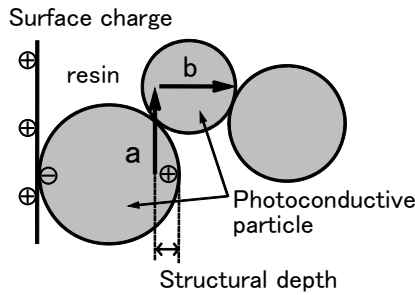


Figure 3. Schematic configuration for structural traps. Arrows a and b indicate directions forward which holes move.

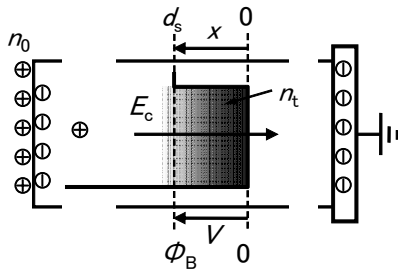


Figure 4. A generalized structural trap model.

Fig. 4 shows a generalized structural trap model, where  $d_s$  is the average of structural depths of individual particles,  $E_c$  is the electric field due to the surface charges  $n_0$  and reminded holes and  $n_t$  is the trapped holes ( $\text{cm}^{-2}$ ). The Maxwell-Boltzmann distribution is applied to trapped holes as follows:

$$f(v) dv = \left( \frac{m}{2\pi kT} \right)^{0.5} \exp\left(-\frac{mv^2}{2kT}\right) dv \quad (1)$$

where  $m$  is the hole mass,  $k$  is the Boltzmann constant, and  $T$  is the absolute temperature in Kelvin. Assuming that the contact point to the next photoconductive particle is closer to unit, one dimensional and + directional motion is taken into account.

The energy barrier  $\Phi_B$  at the distance  $d_s$  shown in Fig. 4 is calculated using a method of successive calculation with  $E_c$ , eq. (1), trapped holes  $n_t$  and Gauss's law. The detrapping rate of holes with kinetic energy higher than  $\Phi_B$  is given by

$$\frac{dn_{dt}}{dt} = -n_t \left( \frac{kT}{2\pi m} \right)^{0.5} \exp\left(-\frac{\Phi_B}{kT}\right) \quad (2)$$

### Photo-induced discharge mechanism

The photo-induced discharge model for the high gamma photoreceptors is schematically illustrated in Fig. 5. Structural trap layers distribute periodically in the photoconductive layer and the distances between structural trap layers are the mean free path of holes.

The energy barrier  $\Phi_{B0}$  shown in Fig. 5 (a) is related to the initial surface potential  $V_0$  by the equation

$$\Phi_{B0} = V_0 d_s / d_p \quad (3)$$

where  $d_p$  is the thickness of the photoconductive layer.

The quantum efficiency of the field controlled carrier photo-generation of x-type metal-free phthalocyanine is reported by Hackett [9] as follows:

$$\eta(E) = \eta_0 \exp[(\beta_{pf} E^{0.5} / kT) - (\Phi_{0pf} / kT)] \quad (4)$$

where  $E$  is the electric field, and  $\beta_{pf} = 1.06 \times 10^{-4} \text{ eV} \cdot \text{cm}^{0.5} \cdot \text{V}^{-0.5}$ ,  $\Phi_{0pf} = 0.09 \text{ eV}$  for the wavelength of 620 nm. We added the correction term  $\eta_0$  to Hackett's equation considering the difference of wavelengths and/or sample preparations.

Photogenerated holes  $n_g(t)$  are trapped by the first structural trap during the induction period as shown in Fig. 5 (b). The energy barrier of the structural trap  $\Phi_B$  decreases as the exposure time proceeds, finally trapped holes begin to detrapp. Detrapped holes  $n_{dt}$  are given by eq. (2). The instantaneous trapped hole carrier density  $n_t(t)$  is determined as follows:

$$n_t(t) = n_g(t) - n_{dt}(t) \quad (5)$$

The structural traps within the photoconductive layer during the carrier transport are shown in Fig. 5 (c). Assuming that total number of structural trap layers are  $N_L$ , detrapped holes  $n_{dtN}$  ( $N \geq 2$ ) are given by eq. (2), then, the trapped hole carrier density in the  $N$ th structural trap layer  $n_{tN}$  is determined as follows:

$$n_{tN}(t) = n_{dt(N-1)}(t) - n_{dtN}(t) \quad (6)$$

Therefore, the surface potential  $V_{tN}$  due to holes at the  $N$ th structural trap layer can be given by

$$V_{tN}(t) = e n_{tN}(t) d_p (1 - N/N_L) / \epsilon_r \epsilon_0 \quad (7)$$

Therefore, the instantaneous surface potential of the photoconductive layer  $V_s(t)$  is calculated by

$$V_s(t) = V_0 - \frac{e n_g(t) d_p}{\epsilon_r \epsilon_0} \frac{N_L}{N=1} + \sum V_{tN}(t) \quad (8)$$

The solid curve shown in **Fig. 1** was calculated using the method of successive calculation with eqs. (3) ~ (8) and  $d_s = 0.02 \mu\text{m}$ . The correction factor and the structural trap layers were determined to be  $\eta_0 = 0.88$  and  $N_L = 15$  layers (the distance between structural trap layers =  $1.2 \mu\text{m}$ ).

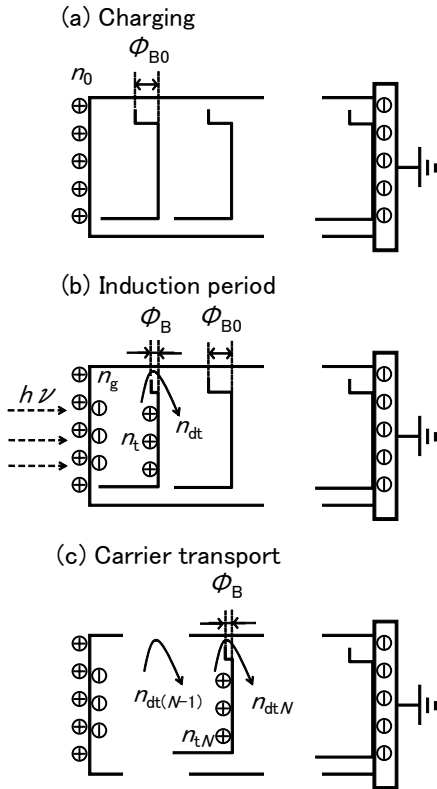


**Figure 5.** Photo-induced discharge mechanism for a high gamma photoreceptor based on the structural trap model.

### Dark discharge mechanism

The dark discharge model for the high gamma photoreceptors is schematically illustrated in **Fig. 6**. Holes and electron charges are thermally generated in the photoconductive layer as shown in **Fig. 6** (a). The negative potential  $V_e$  due to electron space charges is given by

$$V_e(t) = e G t d_p^2 / 2 \epsilon_r \epsilon_0 \quad (9)$$

where  $G$  ( $\text{cm}^{-3} \cdot \text{s}^{-1}$ ) is the thermal carrier generation rate and  $t$  is the time.

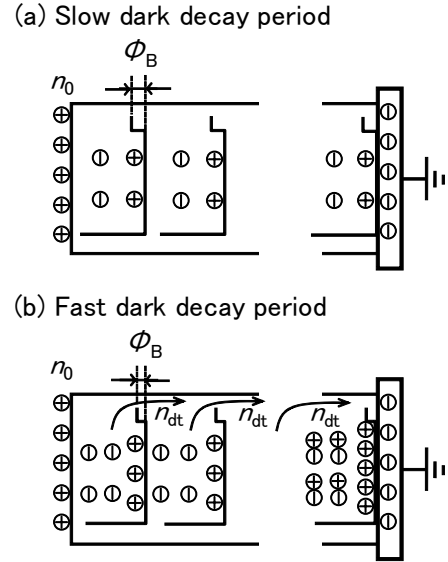


**Figure 6.** Dark discharge mechanism for a high gamma photoreceptor based on the structural trap model.

The instantaneous trapped hole carrier density  $n_t$  is determined as follows:

$$n_t(t) = e G t d_p / N_L - n_{dt}(t) \quad (10)$$

The positive potential  $V_t$  due to trapped holes is given by

$$V_t(t) = \frac{n_t(t) d_p (N_L - 1)}{\epsilon_r \epsilon_0} \quad (11)$$

The surface potential  $V_s$  and the energy barrier  $\Phi_B$  decrease as the dark decay time proceeds as shown in **Fig. 6** (a), finally the trapped holes begin to detrapp from all structural traps as shown in **Fig. 6** (b). The detrapped holes  $n_{dt}$  are given by eq. (2).

The surface potential of the photoconductive layer  $V_s(t)$  is

$$V_s(t) = V_0 - V_e(t) + V_t(t) + V_f(t) \quad (12)$$

where  $V_f(t)$  is the potential due to detrapped holes (details are omitted in this paper).

The solid curve shown in **Fig. 2** was calculated using the method of successive calculation with eqs. (9) ~ (12),  $G = 4.2 \times 10^{13} \text{ cm}^{-3} \cdot \text{sec}^{-1}$ , and  $N_L = 15$  layers. The structural depth was determined to be  $d_s = 0.02 \mu\text{m}$ .

## Electrophotographic performance

### 1. High gamma and high image resolution

The broken line curves in Fig. 1 show photo-induced discharge curves with  $d_s = 0 \mu\text{m}$ ,  $0.01 \mu\text{m}$ ,  $0.015 \mu\text{m}$ ,  $0.03 \mu\text{m}$ . The induction exposure and gamma characteristics are found to be depend on the structural depth. The above investigation leaves big hopes of how high the resolution can be achieved with the **Digital Photoreceptor HGPC**. Fig. 7 (b) shows various dot-per-inch equivalent line pair drawing image on the photoconductor with the laser beam of diameter about  $6 \mu\text{m}$  and developed with the liquid toner. The light pattern on the photo-paper confirms the image as shown on Fig. 7 (a). Although there is some localized unevenness due to the rough surface of the photoreceptor, two image patterns ((a) and (b)) are very similar. Closer observation shows that the 4400 dpi resolution (one-dot line pair) is defined, though the line are bit thin along with the well defined 1467 dpi (3-dot line pair) lines. The **Digital Photoreceptor HGPC** shows that the all images can be displayed correctly.

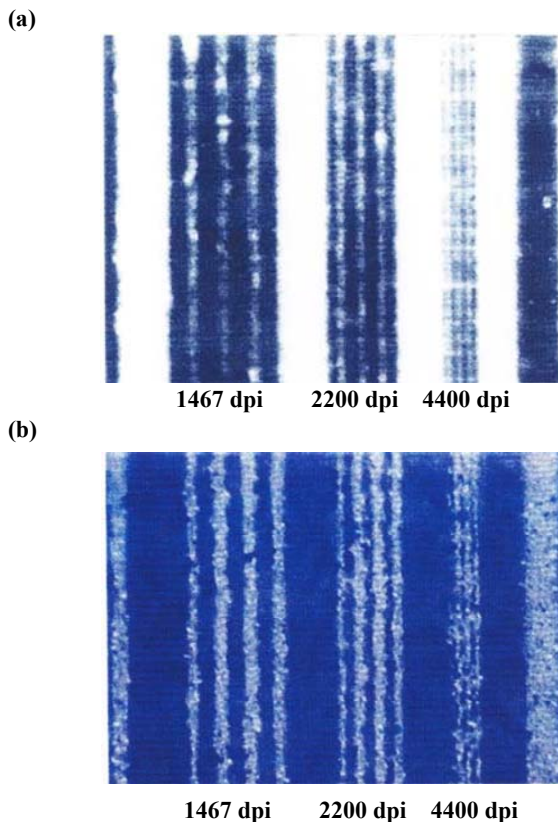


Figure 7. (a) Image on photo-paper and (b) liquid toner image on **Digital Photoreceptor HGPC**.

### 2. Slow dark decay and blocking layer

Eqs. (9) and (11) yield

$$\frac{dV_s}{dt} = \frac{dV_e}{dt} - \frac{dV_t}{dt} = -\frac{e d_p^2 G}{2 \epsilon_r \epsilon_0 N_L} \quad (13)$$

The dark decay rate of a trap free photoreceptor has been theoretically known as the eq. (13) with  $N_L=1$ . Therefore dark decay rates of high gamma photoreceptors are improved to be  $N_L$  times as expressed in eq. (13). It is found theoretically that the slow dark decay rate depends on the limited displacement within  $d_p / N_L$  for thermally generated holes. It also means that structural traps near the surface work as a blocking layer against the injection of charge carriers on the surface of the photoconductive layer.

### 3. Fast photoresponse

The time loss due to trap and detrap processes during carrier transport is calculated to be  $20 \times 10^{-3}$  sec at the exposure of  $1.7 \mu\text{J}/\text{cm}^2$  shown in Fig. 1. It is sufficiently shorter than the time from an exposure position to a development station (about  $0.1 \sim 0.3$  sec). The x-type metal-free phthalocyanine's own photoresponse to digital image exposure is not deteriorated in spite of charge carrier trappings during carrier transport.

## Conclusion

The high gamma photoreceptors are found to be well described by our theoretical model which takes into account the structural trap. We have found that the electrophotographic performance depends on the structural trap. Toners have been already made increasingly fine in diameter. The high gamma photoreceptor is the most promising target for the next generation imaging technology.

## Acknowledgement

The authors would like to acknowledge Dr. Inan Chen who reviews this article and provided valuable suggestions.

## References

- [1] J.W. Weigl, J. Mammino, G. L. Whittaker, R.W. Radler and J.F. Byrne, (Walter de Gruyter Berlin, 1972), pg. 287.
- [2] K. Kinoshita, Jpn P H5-19140 (1993) (in Japanese).
- [3] J. Decker, K. Fukae, S. Johnson, S. Kaieda and I. Yoshida: Proc. IS&T's 7th Intl. Congress on Advances in Non-Impact Printing Technol., pg. 328 (1991).
- [4] K. Kubo, T. Kobayashi, S. Nagae, and T. Fujimoto, Jour. Imaging. Sci. and Technol., **43**, 248 (1999).
- [5] A. Omote, Y. Itoh, and S. Tsuchiya, Jour. Imaging. Sci. and Technol., **39**, 271 (1995).
- [6] T. Kitamura, Y. Miyazawa, and H. Yoshimura, Jour. Imaging. Sci. and Technol., **40**, 171 (1996).
- [7] Y. Hoshino, T. Murata, H. Watanabe and I. Yoshida, Proc. IS&T's NIP16, pg. 129 (2000).
- [8] T. Kurita, Proc. 25th Annual Conference of SEPJ, pg. 7 (1970) (in Japanese).
- [9] C. F. Hackett, J. Chem. Phys., **55**, 3178 (1971).

## Author Biography

Kuniki Seino joined Minolta in 1967 and participated in research and development of photoreceptors such as PVK/Se, CuPc/hydrazone/polymer and CdSnCdCO<sub>3</sub>-resin. He received his Dr. Sc. in Physics in 1972 from the Kwansei Gakuin University in Japan. He managed groups responsible for the commercialization of copy machine series. He was named a Senior member of the IS&T in 2002. He was awarded the ISJ Journal Award in 2001. He joined Afrit Corporation as a consulting scientist in 2005.